SEMARAK ILMU PUBLISHING

Journal of Advanced Research in Fluid Mechanics and Thermal Sciences

Journal homepage:
https://semarakilmu.com.my/journals/index.php/fluid_mechanics_thermal_sciences/index
ISSN: 2289-7879

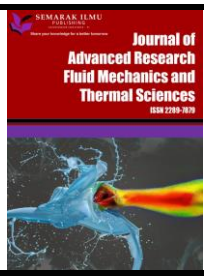

The Aerodynamic Characteristics Investigation on NACA 0012 Airfoil with Owl's Wing Serrations for Future Air Vehicle

Muhammad Ridzwan Ramli[1], Wan Mazlina Wan Mohamed[1,*], Hamid Yusoff[2], Mohd Azmi Ismail[3], Ahmed Awaludeen Mansor[2], Azmi Hussin[2], Aliff Farhan Mohd Yamin[2]

[1] Malaysia Institute of Transport (MITRANS), College of Engineering, College of Engineering, Universiti Teknologi MARA Shah Alam, 40450 Shah Alam, Selangor, Malaysia
[2] Center for Mechanical Engineering Studies, Universiti Teknologi MARA, Cawangan Pulau Pinang, 13500 Permatang Pauh, Pulau Pinang, Malaysia
[3] School of Mechanical Engineering, Universiti Sains Malaysia, 14300, Nibong Tebal, Pulau Pinang, Malaysia

ARTICLE INFO

Article history:
Received 25 July 2022
Received in revised form 9 December 2022
Accepted 21 December 2022
Available online 8 January 2023

Keywords:
Aerodynamic performance; noise reduction; silence flight; wing serrations

ABSTRACT

Owls have an incredibly unique ability to fly in silence, and this ability has significant potential to reduce noise pollution from aircraft engines. For decades, researchers have been studying the noise abatement system in conventional aircraft, but only a few of them had looked into the owl's ability to reduce the aircraft noise level, especially on the serrated wing. The present study aims to investigate the lift and drag coefficient of the serrated wings including leading-edge serrations, trailing-edge serrations, both-edge serrations, and the original/baseline wing model from the NACA 0012 airfoil. The experimental testing was performed in a wind tunnel at Reynolds numbers of 20,000 and 40,000 and angle of attack from 2° to 30°, in 2° angle intervals. In general, the results showed that each wing model produced a similar lift and drag coefficient profiles, which were proportional to the angle of attack. At Reynolds number of 40,000, the lift coefficient increases from 0.45 to 1.5, as the angle of attack increases from 2° to 24°. Afterward, it decreased as the angle of attack exceeded 24°. According to the data, the trailing-edge serrations model showed the lowest drag coefficient at a Reynolds number of 40,000. Meanwhile, the highest lift coefficient at Reynolds number of 40,000 had been produced by the baseline wing model. This result is beneficial in reducing the noise generation produced by wing structure and at the same time enhancing aerodynamic efficiency.

1. Introduction

The aircraft industry has taken many years of development to achieve advanced technologies to date. In the earliest year of the emerging flying technology, the wings have only been designed in a flat shape. Then, as humans began to develop a comprehensive understanding from time-to-time, the wing with flat shape has altered into the design called airfoil shape. Airfoil is defined as the cross-sectional shape of the wing. The airfoil-shaped wing has been used as aerodynamic aids for aircraft

* *Corresponding author.*
E-mail address: wmazlina@uitm.edu.my

https://doi.org/10.37934/arfmts.102.1.171183

lift and thrust performances. Moreover, as the commercial flight's speed increase up to subsonic flow, the aerodynamic characteristics study become essential especially in aircraft critical components including wings and nacelle. Besides the engine, the wing profile also contributes to aircraft noise pollution. The high drag friction of the wing has caused vibration and is producing noise, especially if the wing vibrate in its natural frequency. The noise produced by the commercial aircraft is significant cause to adverse reaction related to the operation of flight. It leads the Federal Aviation Administration (FAA) to urge all aircraft manufacturers to increase noise abatement system [1].

The noise generation mechanisms in an aircraft are related to aerodynamics, propulsion and their interactions. Aircraft noise prediction has been developing through the years by certifying the level of maximum exposure and by imposing new reduction targets for the next decade. In 1970s, 7 million people were subjected to high noise level from aircraft. This statistic is increasing each year. According to FAA, the rate of people exposed to aircraft noise increases severely from 2012 to 2017. The new case of people exposed to the noise in 2012 were 315000, and this value increase up to 408000 in 2017 [2]. Aircraft engine has been identified as the major contributor of aircraft noise. Aircraft noise becomes critical during take-off and approach phases, as this noise affect flight passengers, airport crews and surrounding community. Acoustic liner (AL) has been introduced and installed in the nacelle inlet zone, and chevron nozzle has been applied in nacelle trailing edge, in order to reduce engine noise. However, AL alone is not enough, noise abatement system must be installed underneath nacelle lip-skin. Thus, bias acoustic liner (BAL) has been introduce to overcome noise and ice accretion problems [3]. Moreover, the bias flow from BAL reduces drag coefficient of the nacelle and aircraft [4].

Many researchers have study BAL, as an alternative noise abatement system. In 2003, a study had been conducted to investigate absorption ability of axial acoustic wave by perforated liner with bias flow [5]. Then, with the help of CFD, the thermal performance of BAL had been conducted in 3D [6]. In case low or no bias and glazing flows, the main characteristic that influence the performance of noise abatement system is frequency. However, when the glazing flows is taken into account, meaning bias flow greater than amplitude of acoustic velocity in the orifice, the Mach number of bias flow affect noise abatement performance [7].

Besides enhancing noise abatement system in the nacelle, the design and material of wing also impacted on aircraft noise. One of the advanced technologies in aircraft is the introduction of micro air vehicles (MAV). The MAV is compact and can operate automatically by handling from the ground regulatory pilot that brings an ability to fly in confined areas or in a harmed area that is not suitable for physical observation [8]. In MAV application, the noise is produced by wing, especially for flapping wing. The inspiration that can be made to improve the aerodynamic performance of the flying mechanism in terms of reducing the noise level is needed to refer to the mother of nature, such been done by several researchers to discover new knowledge and technology, like the inspiration of bald eagle to reduce the influenced of induced drag from flying wing [9]. Thus, the study of the owl's wing shape or chevron might be useful in solving the issue related to noise generation by wing structures [10, 11]. The Owl's wing has special characteristics; unusual wing morphologies. They are commonly recognized for their ability to fly in almost absolute silence, achieving exceptionally low noise gliding and flapping flights [12]. During gliding or flapping flight, they may suppress the wing-induced aerodynamic sound to an incredibly low level of a frequency below 2 kHz, enabling them to easily target prey including mice and voles [13].

Klaas *et al.,* [14] claimed that most owls have evolved unique wing adaptations to meet the silent flight requirements. The owl wing has comb-like structure, soft, and porous [15]. In addition, the barn owl is stated to be capable of suppressing and reducing the wind-induced aerodynamic sound, especially in gliding or flapping flight conditions [13]. Since the owl's wing features has many

advantages in enhancing noise abatement system, the chevrons or serrated edges are applied on nacelle trailing edge for Boing 777-300ER with GE-115B engines [16]. Moreover, the CFD simulation data showed that the chevron nozzle for nacelle has 2% higher maximum thrust than the translating nozzle technique [17].

Based on the literature survey above, most of the noise abatement system including AL, BAL, and chevron nozzle trailing edge had been applied in nacelle and aircraft engine. Most of the study applied noise abatement system on nacelle or aircraft engine. Only a few researchers employed this system on the wing. Nowadays, unmanned aerial vehicles (UAVs) and MAVs are getting popular among researchers. The results of aerodynamic performance of chevron wing including lift coefficient (C_L) and drag coefficients (C_D), are hard to find in the literature. Other than that, the serrated wing has a good potential to improve the aerodynamic performance as well as in reducing the sound emission compared to the clean or conventional wing. However, those researchers have only been done on a single type of serrations (i.e.; either leading-edge serrations, trailing-edge serrations or fringe-type trailing-edge extension). In addition, an integration of multiple types of serrations has not been done yet in a detailed manner. Therefore, the paper presents the C_L and C_D of chevron or serration wings against angle of attack (*AoA*), at two different Reynolds number (*Re*). The purpose of the present study is used for UAVs application, which implemented the flight circumstance of the UAVs regime.

2. Methodology

2.1 Model Development

The present work studied 4 serration wing models named leading-edge serrations (LE), trailing-edge serrations (TE), both-edge serrations (BE) and original/baseline (BL) model, as illustrated in Figure 1. The geometric modelling was developed using Catia V5 CAD, and the models were fabricated by Computer Numerical Control machine (CNC). Aluminium was used as model material since it has low density.

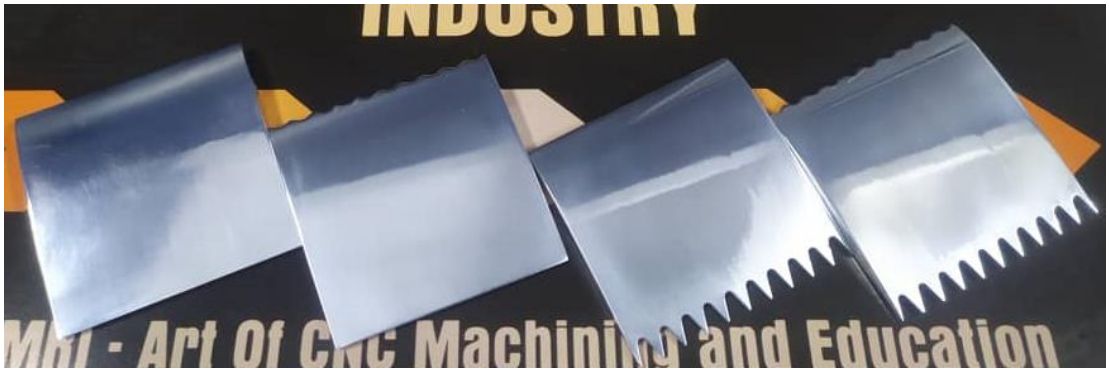

Baseline model (BL)	Leading – edge serration model (LE)	Trailing– edge serration model (TE)	Both–edge serration model (BE)

Fig. 1. Wing model of the study

The dimensions of the model were 50mm x 50mm and 6mm, as illustrated in Figure 2. At the leading edge of LE and BE wing models, the serration parameter was at 5 mm wavelength (λ) and 1.5 mm amplitude (h) while at trailing edge for TE and BE wing models, the serration parameter was at 5 mm of λ and 8 mm of amplitude (H). All the wing models had been polished three times where the special polishing fluid was spread evenly on the surface using Bench Polishing Machine, in order to obtain a smooth surface. The polishing proses reduced the surface roughness of the wing model, then reduced the drag coefficient of the wing.

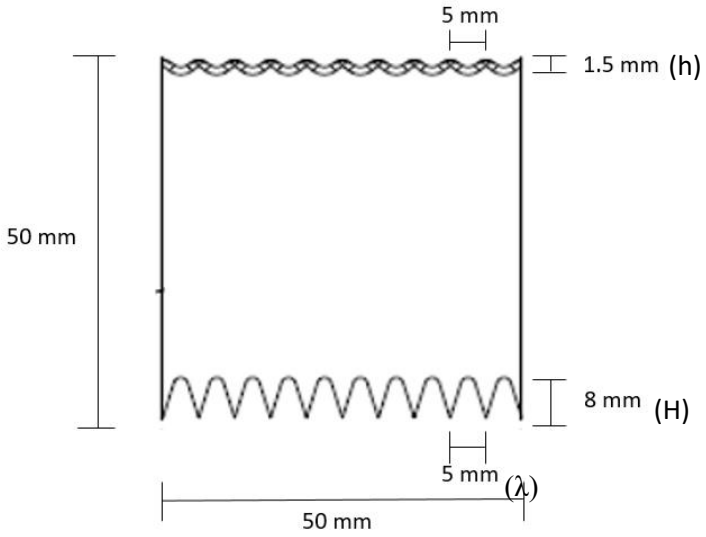

Fig. 2. The dimension of BE wing model

Furthermore, the M4 threaded bore with 10 mm depth were made at the left side of the experimental model as the connecting element to the balancing force. The M4 was design exactly at quarter of 12 mm from the leading edge of every experimental model. While in the wind tunnel case, the experimental model was mounted horizontally at the center of the wind tunnel facing directly to the flow stream. The M4 threaded bore was mounted using a 100 mm connecting rod into the measurement setup outside the wind tunnel. Table 1 summarised the wing model dimension, which the experimental model with leading-edge serration will have a sinusoidal shape of serration while the model with trailing edge serration will have a sawtooth shape.

Table 1
The summaries of Wing Models dimension

Wing Model	Leading-Edge serration type	Trailing-Edge serration type	Leading-Edge λ (mm)	Leading-Edge h (mm)	Trailing-Edge λ (mm)	Trailing - Edge h (mm)
BL	-	-	-	-	-	-
LE	Sinusoidal	-	5	1.5	-	-
TE	-	Sawtooth	-	-	5	8
BE	Sinusoidal	Sawtooth	5	1.5	5	8

2.2 Experimental Setup

The experiment had been conducted at School of Aerospace Engineering, Universiti Sains Malaysia. The closed circuit subsonic incompressible wind tunnel was used to supply air flow to the experiment. The wind tunnel facility that been utilized for this experimental research has a capability

to supply the air flow up to 25 ms^{-1}. Meanwhile, in this experimental research conducted two different air velocities; 7.9m $s^{-1}$and 11.84m s^{-1}, represented Re of 20,000 and 40,000, respectively. The dimension of test section of wind tunnel was 30cm x 30cm x 50cm. Other than that, the other property which influenced in this experimental study is utilized 1.172kg/m^3, 1.15868 x 10^{-5} m^2/s and 26.8°C, which represented the density, viscosity, and temperature for this research, respectively. Besides, the air flow in this experimental research was assumed to be laminar flow as the Re for the experimental model was conducted much smaller than Re 500,000 [4]. Next, Figure 3 and Figure 4 showed the setup of the experiment work, respectively.

In order to run the experimental research for this study, the wing model was connected to the balancing unit using small and light rod to the threaded bore that been produced in the fabrication stage on the left side of every experimental specimens. Then, balancing unit contained strain gauge was used to measure lift and drag forces generated by this research on the serrated wing profile imitated from natural creatures. The data acquisition (DAQ) was used to convert physical signal from balancing unit to digital signal. The DAQ was connected to the computer through universal serial bus (USB) standard A-B cable. After that, Lab View software and computer were used to analyse the data from DAQ, and recorded in the computer hard disk. Before the experiment started, the balancing unit and DAQ were calibrated using weight load tester to make sure the precision of the generated result. Figure 5 shows DAQ device was used in the experimental study. Pitot tube and digital manometer were also used to measure air velocity inside the wind tunnel.

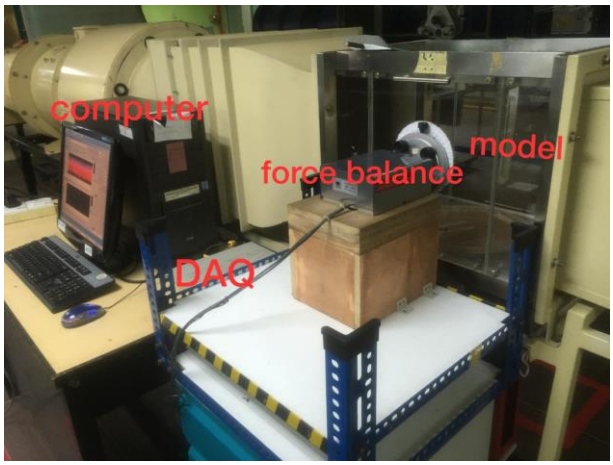

Fig. 3. The experimental setup in wind tunnel

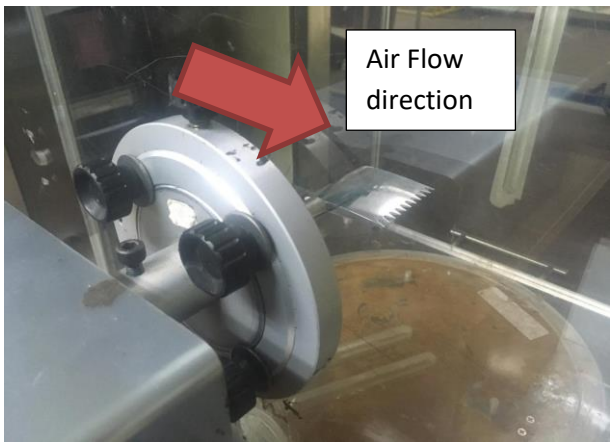

Fig. 4. Side view of wing model in the wind tunnel

Fig. 5. Kyowa PCD-300A data acquisition system

2.3 Data Reduction and Operating Condition

The experiment was conducted for two different *Re*; 20,000 and 40,000. Reynolds number is the ratio between inertial forces to viscous forces with general equation as stated in Eq. (1) [18]. In the wing study, the hydraulic diameter for wing is cord length (c). Then, the *Re* is rewrite as Eq. (2).

$$Re = \frac{U_\infty D_H}{v} \tag{1}$$

$$Re = \frac{cU_\infty}{v} \tag{2}$$

where, v is the kinematic viscosity of air, D_H is the hydraulic diameter, U_∞ is wind tunnel air velocity, and *c* is chord wing

Lift coefficient (C_L) and drag coefficient (C_D) are described instead of lift and drag forces because lift and they are dimensionless characteristic, and independent from size. C_L and C_D in the present work are calculated by Eq. (3) and Eq. (4), respectively.

$$C_L = \frac{2F_L}{\rho\, x\, U_\infty x\, A} \tag{3}$$

$$C_D = \frac{F_D}{\frac{1}{2}\rho {U_\infty}^2 A} \tag{4}$$

where, F_L is the lift force, F_D is the drag force, ρ is the air density and A is the projection of wing surface area.

The experiment covered the angle of attack (*AoA*) from 2° to 30°, with 2° angle interval. The *AoA* was controlled by *AoA* transducer with a precision of 1°, which had been installed in the wind tunnel test section. Table 2 summarised the operating conditions in the present work.

Table 2
Parameters of the experimental study

Wing Models	*Re*	*AoA* (°)
BL, LE, TE, BE	20,000, and 40,000	2, 4, 6, 8, 10, 12, 14 16,18, 20, 22, 24, 26, 28, and 30

3. Results and Discussion

The effect of *AoA* from 2° to 30° on C_L and C_D were discussed below. The discussion covered 2 different *Re*; 20,000 and 40,000. The air properties were taken in room temperature; T_∞ =28.6°C.

3.1 Effect of Wing Serrations on Lift Performance as Function of AoA

Figure 6 and Figure 7 showed the effect of *AoA* on C_L at Re of 20,000 and 40,000, respectively. In general, both figures showed the increasing of C_L relative to *AoA* increased until it reaches stall angle. As *AoA* exceeded stall angle, the C_L decreased to *AoA* of 30°. It was expected that C_L inversely proportional to *AoA* at *AoA* beyond 30°. As shown in Figure 6, BL, LE and TE models produced similar C_L profile against *AoA*, and they were hard to distinguish one to the others. The lowest C_L was produced by BE model. The C_L of BL model increased from 0.45 to 1.75, as the *AoA* increased from 2° to 24°, which was the highest C_L at *Re* 20,000. The fluctuation of C_L in Figure 6 might be due to high turbulent intensity as the experiment were conducted in the low air velocity.

Figure 7 shows a smooth profile for all models, except TE model. All models showed the same profile pattern, which were directly proportional to *AoA* until they reached a stall angle. As *AoA* exceeded stall angle, contrary to Figure 6, the C_L in Figure 7 begin to fluctuate until AoA 30°. Along with *AoA*, BL model shows the highest C_L and followed by TE model and LE model. The lowest C_L was produced by BE model. BE model showed the lowest C_L at *AoA* of 2°. Subsequently, C_L of BE model increased up to 1.2 at *AoA* of 26°. Unlike the other models, the C_L BE model increased up to 1.3 as *AoA* increases to 30°. However, the C_L of BL model showed the highest number at *AoA* of 2°. Then, the C_L increased up to 1.5, as *AoA* has approached stall angle at 26°. Afterwards, the C_L fluctuated until *AoA* reached 30°. In addition, according to both Figure 6 and Figure 7, TE wing model generated higher C_L than LE and TE wing models but still lower than BL wing model.

Analysis showed that BL model have the highest C_L. A potential reason was that BL leading-edge and trailing-edge have not changed. Therefore, the air flowed smoothly over BL surface with uniform pressure distribution. The lower C_L for LE wing model because of the serrations' amplitude, λ = 5mm was larger than the original serrations of an actual owl's wing. The wing of an owl has a special serration that help to smoothen the airflow when in contact with the wing surface. Thus, the LE model reduced the maximum lift since it had obstructed the air flow over model surface. Thus, the air pressure distribution on the model surface body was inconsistent than in BL model pressure distribution.

The lift performance for TE wing model was higher than LE wing model because TE leading-edge was not disturbed the air flow over the model surface. However, TE had a lower C_L than BL model due to the location of separation point for TE where it might be changed either to the leading or trailing edge. This is because the pressure distribution on trailing edge surface was less uniform due to serration design at the trailing edge. The implementation of trailing-edge serrations didn't elevate the coefficient of lift. Moreover, the combination of both leading-edge and trailing-edge serrations on BE wing, it lowers the C_L even more, thus C_L of BE is the lowest in the present study. Furthermore, the research conducted by Yong *et al.,* [19], revealed that the serrations geometry at the wing structure are capable to reduce the maximum lift coefficient from 12° to 15° over the critical angle region, but increased the lift output in the deep stall region, which from 17° to 20° for the application of symmetrical airfoil.

Next, Table 3 summarised C_L performance for all models in the experimental study. TE model shows only 6.2% and 2.6% lower C_L than BL at *Re* of 20,000 and 40,000, respectively. At *Re* of 40,000,

BE model produced C_L 26.9% lower than BL. In conclusion, BE produces the lowestC_L, followed by LE and TE models. BL shows the highest C_L in the present work.

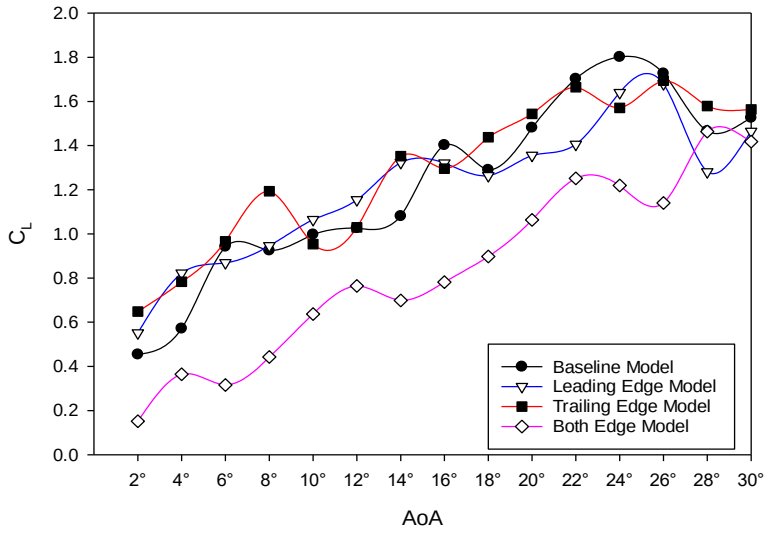

Fig. 6. C_L versus *AoA* for (*Re* = 0.2 x 105)

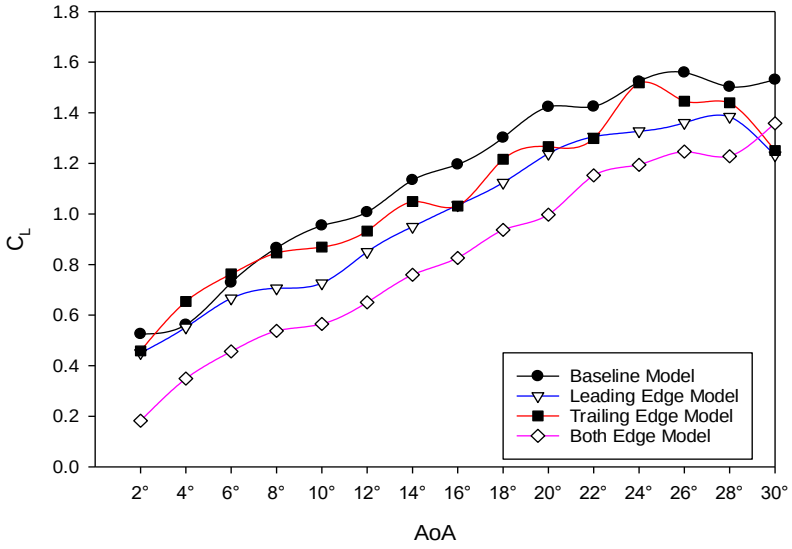

Fig. 7. C_L versus *AoA* for (*Re* = 0.4 x 105)

Table 3
$C_{L\,max}$ comparison and Percentage Reduction to BL Model

Wing Model	$C_{L\,max}$, $Re = 0.2\,x\,10^5$	Percentage Reduction (%)	$C_{L\,max}$, $Re = 0.4\,x\,10^5$	Percentage Reduction (%)
BL	1.802	-	1.56	-
LE	1.680	6.9	1.44	7.7
TE	1.690	6.2	1.52	2.6
BE	1.464	18.8	1.36	26.9

3.2 Effect of Wing Serrations on Drag Performance as Function of AoA

Figure 8 and Figure 9 show the relationship between C_D and AoA at Re of 20,000 and 40,000, respectively. Both figures show that, the C_D for all model proportional to AoA. At Re of 20,000, BE

model provided the highest, followed by LE, TE and BL model. As shown in Figure 8, BE model shows the C_D of 1.0, which was the highest in the present study. Then C_D for BE increased up to 1.6, as AoA increases to 28°. The figure also showed that BE model presented the lowest C_D along AoA, except for AoA of 24°. The C_D of BE had increased from 0.1 to 0.95, as the AoA increased from 2° to 30°. The maximum C_D for BE was 0.65 higher than that of BL.

In Figure 9, TE model produced the lowest C_D along AoA, and the highest C_D was provided by BL model. The highest C_D gradient was generated by BL model. At AoA of 2°, the C_D difference between BE and BL around 0.5. Then, the C_D difference between BE and BL model decreased to 0.02. Figure 9 also shows that, C_D for LE lower than BL, however, it was higher than TE model. The highest C_D for Re of 40,000, was recorded by BL model, at AoA of 30°.

Table 4 summarised the C_D for all the studied models at Re of 20,000 and 40,000. At Re of 20,000, BE models had 59.8% higher maximum C_D than BL. Moreover, TE showed 3.92% higher maximum C_D than BL did. On the other hand, at Re of 40,000, TE model produced maximum C_D lower 18.75% than BL model. In addition, BE had a maximum C_D 1.56% which was lower than BL model did. This result supported by Roa *et al.,* [13] and Klän *et al.,* [14] agreement in their report.

At low Re, the serrations edge showed no significant effect to reduce drag coefficient. BL model still produced the lowest C_D. However, at higher Re, TE model successfully lowering the C_D compared to the BL model. It happened due to the trailing-edge serrations that provided a higher-pressure distribution at trailing surface. This situation also been supported by the study conducted by Yong *et al.,* [19], which found that the aerodynamic lift and drag measurement on the symmetric NACA 0012 airfoil displayed significantly different behaviour compared to that of the asymmetric NACA 65-(12)10 airfoil. The serration NACA 0012 airfoil generally developed a lower drag than the baseline airfoil especially at the high Re.

Other than that, Usama *et al.,* [20], revealed that due to the vortex formation in the wake blunt regions formed by serrated structures, the introduction of serration also increases the C_D. The sole explanation for the rise in drag is an increase in bluntness due to an increase in serration depth. Therefore, the geometry of the serrations depth also influenced the generated result from the study. As a consequence, the separation point location changed, perhaps downward to trailing edge, which helped in reducing trailing-edge vortices.

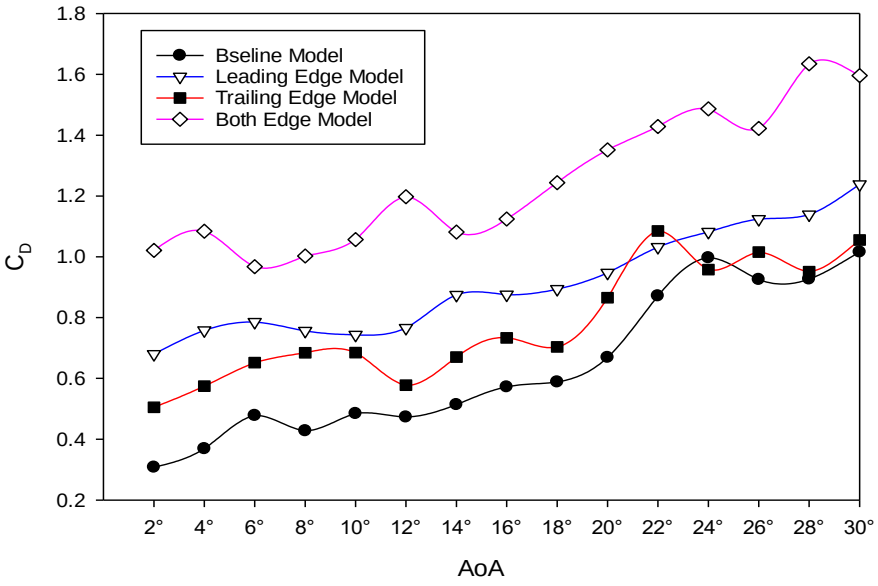

Fig. 8. Coefficient of drag versus angle of attack graph (Re = 0.2 x 105)

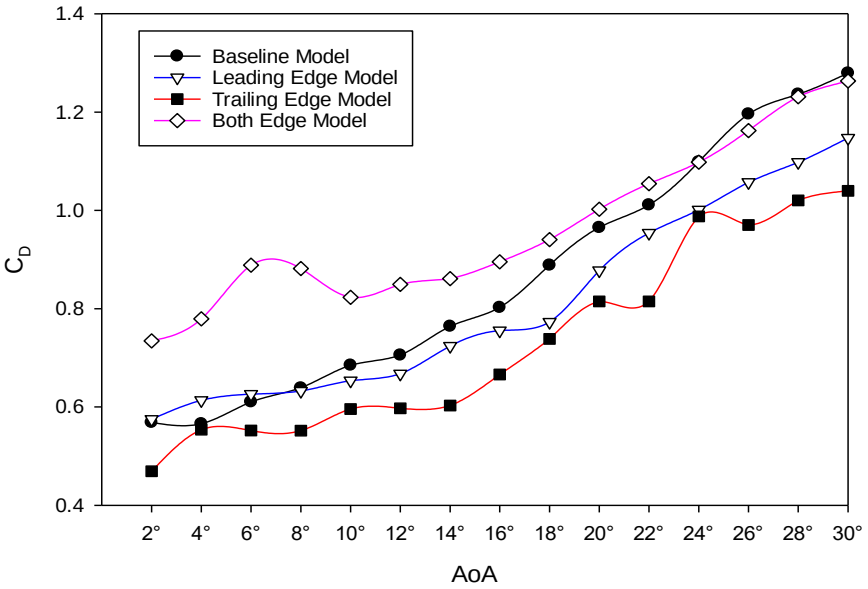

Fig. 9. Coefficient of drag versus angle of attack graph (Re = 0.4 x 105)

Table 4
$C_{D\ max}$ comparison and Percentage Reduction to Baseline Model

Wing Model	$\boldsymbol{C_{D\ max}}$, $\boldsymbol{Re = 0.2\ x\ 10^5}$	Percentage Reduction (%)	$\boldsymbol{C_{D\ max}}$, $\boldsymbol{Re = 0.4\ x\ 10^5}$	Percentage Reduction (%)
BL	1.02	-	1.28	-
LE	1.24	-21.57	1.15	10.16
TE	1.06	-3.92	1.04	18.75
BE	1.63	-59.8	1.26	1.56

3.3 Effect of Wing Serrations on Lift-To-Drag Ratio as Function of AoA

Figure 10 and Figure 11 show the relationship between *lift-to-drag ratio* and *AoA* at *Re* of 20,000 and 40,000 respectively. Both figures show that, the *lift-to-drag ratio* for all model proportional to *AoA*. From Figure 10, which relative to the *lift-to-drag ratio* for *Re* of 20,000 illustrated that the BL model show the highest reading compare to the other three model with serration. The highest *lift-to-drag ratio* that been recorded from the experimental works conducted in this study at *Re* of 20,000 is achieved at *AoA* of $16°$, which represent the *lift-to-drag ratio* around 2.47 respectively. Meanwhile, if referring to the Figure 11 which representing the *lift-to-drag ratio* for *Re* of 40,000, it illustrated the other trend which the most beneficial model that capable to reduce the noise and at the same time provide the good aerodynamic characteristics for the serrated application is trailing-edge (TE) model. TE model not just capable to reduce the intensity of noise generation, but at the same time capable to enhancing the aerodynamic performance which significantly to the other experimental models including the baseline model. The TE model had been recorded providing the highest *lift-to-drag ratio* relative to *AoA* at $14°$ which 1.74469. Besides that, for both edges (BE) model, it shows the lower value of *lift-to-drag ratio* for the both airstream applications.

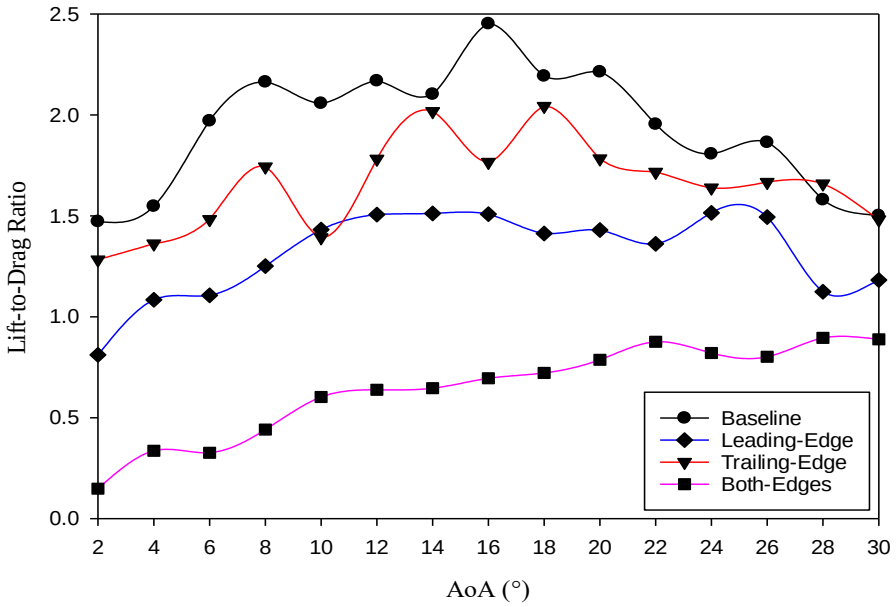

Fig. 10. *Lift-to-drag ratio* versus angle of attack graph for *Re* 20,000

In general, aerodynamic noise is a phenomenon associated with high-speed operation. As speed increases, noise inevitably also increases. Aerodynamic sources of noise differ from the others, which are due to vibrating solid surfaces. Therefore, the noise generated by the airplane when it is hovering or gliding will influence the generated lift and drag as well as the lift-to-drag ratio. In airplane application, the aerodynamic noise is produced by the generation of the total drag, which combination of parasite drag and induced drag. The aerodynamic noise is generated from the vibration when the airflow passes through the wing structures. Thus, the lift and drag coefficient of the flight mechanism will be affected by the noise generation or reduction, respectively. The drag coefficient could be reduced with a reduction of the level of aerodynamic noise since it was influenced by the presence of total drag. It also means that the lift-to-drag ratio also will be enhanced due to the reduction of the total drag of the flying mechanism.

From this experimental study, it can be conclude that the serrated wing model is suitable to apply for the high speed application rather than the low speed application, which TE model show the most capable model in term of reducing the noise generation and at the same time enhancing the aerodynamic efficiency compare to another conducted model including the baseline model. Meanwhile, the serrated application for both-edges (BE) is show significantly low in term of aerodynamic efficiency compare to the other serrated wing models and it represent the worst serration application on the wing structure in term of the aerodynamic efficiency.

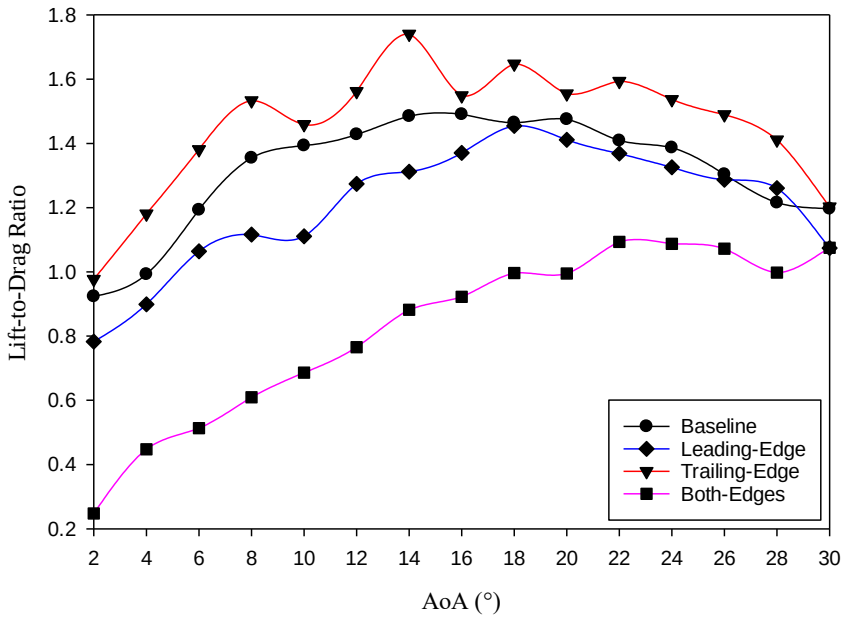

Fig. 11. *Lift-to-drag ratio* versus angle of attack graph at *Re* 40,000

4. Conclusions

The NACA 0012 airfoil with different serrations designs; BL, LE, TE and BE, had been studied to investigate the lift and drag coefficients. The first conclusion that can be drawn from this study is the lift and drag coefficient were proportional to *AoA* for all experimental analysis. Next, BL model showed the highest C_L, and the lowest C_L was produced by BE model. At *Re* of 40,000, the highest C_L for BL, LE, TE and BE are 1.56, 1.44, 1.52 and 1.36, respectively. In addition, TE model had the lower C_D at RE 40,000. TE model showed the maximum C_D, 18.75% lower than BL model. Thus, the serrations design was only effective for aerodynamic efficiency at higher *Re*, *Re* of 40,000. However, at low *Re*, *Re* of 20,000, BL showed greatest aerodynamic efficiency than the other studied models.

Besides that, the serrations study that has been conducted is not only beneficial in order to enhance the lift performance and reducing the drag coefficient of the flying mechanism but the serrations application is also beneficial to the environment. As we have known the world had faced noise pollution that has been contributed by a lot of industries, and one of them is the aircraft industry. This application of the serrations is capable of significantly reducing the level of aerodynamic noise that is hard to tackle before. The suggestion for further study in the serrations application for aircraft application is conducting the study on the serrations wing at high *Re* using a numerical method to visualize the flow pattern of the airstream when it passing through the serrations structure. This effort will give a new idea and knowledge in term of visualisation of the airstream through the serrated wing, which can lead other researcher to continue the study in reducing the noise pollution and at the same time makes a flight mechanism more effective.

Acknowledgement

The authors would like to acknowledge the financial support from Malaysia Institute of Transport (MITRANS) and Universiti Teknologi MARA Shah Alam, Selangor.

References

[1] Ismail, Mohd Azmi, and Jian Wang. "Effect of nozzle rotation angles and sizes on thermal characteristic of swirl anti-icing." *Journal of Mechanical Science and Technology* 32 (2018): 4485-4493. https://doi.org/10.1007/s12206-018-0845

[2] Huerta, M. (2017) *Performance And Accountability Report 2017*. U.S.Department of Transportation Federal Aviation Administration.
[3] Ives, Anthony O., Jian Wang, Srinivasan Raghunathan, and Patrick Sloan. "Heat transfer through a single hole bias flow acoustic liner." *Journal of thermophysics and heat transfer* 25, no. 3 (2011): 409-423. https://doi.org/10.2514/1.t3637
[4] Khai, Lee Chern, Mohd Azmi Ismail, Qummare Azam, and Nurul Musfirah Mazlan. "Experimental study on aerodynamic performance of nacelle lip-skin bias flow." *Journal of Mechanical Science and Technology* 34 (2020): 1613-1621. https://doi.org/10.1007/s12206-020-0323-0
[5] Eldredge, Jeff D., and Ann P. Dowling. "The absorption of axial acoustic waves by a perforated liner with bias flow." *Journal of Fluid Mechanics* 485 (2003): 307-335. https://doi.org/10.1017/s0022112003004518
[6] Ives, Anthony, Jian Wang, Srinivasan Raghunathan, Emmanuel Benard, and Patrick Sloan. "Three dimensional numerical solution of heat transfer in a honeycomb cell." In *7th AIAA ATIO Conf, 2nd CEIAT Int'l Conf on Innov and Integr in Aero Sciences, 17th LTA Systems Tech Conf; followed by 2nd TEOS Forum*, p. 7825. 2007. https://doi.org/10.2514/6.2007-7825
[7] Lawn, Chris. "The acoustic impedance of perforated plates under various flow conditions relating to combustion chamber liners." *Applied Acoustics* 106 (2016): 144-154. https://doi.org/10.1016/j.apacoust.2016.01.005
[8] Mohamed, Wan Mazlina Wan, Mohd Azmi Ismail, Muhammad Ridzwan Ramli, Aliff Farhan Mohd Yamin, Koay Mei Hyie, and Hamid Yusoff. "Experimental Study of Rigid and Flexible Tandem Wing for Micro Aerial Vehicle." *Journal of Advanced Research in Fluid Mechanics and Thermal Sciences* 85, no. 2 (2021): 33-43. https://doi.org/10.37934/arfmts.85.2.3343
[9] Yusoff, Hamid, Koay Mei Hyie, Halim Ghaffar, Aliff Farhan Mohd Yamin, Muhammad Ridzwan Ramli, Wan Mazlina Wan Mohamed, and Siti Nur Amalina Mohd Halidi. "The Evolution of Induced Drag of Multi-Winglets for Aerodynamic Performance of NACA23015." *Journal of Advanced Research in Fluid Mechanics and Thermal Sciences* 93, no. 2 (2022): 100-110. https://doi.org/10.37934/arfmts.93.2.100110
[10] Wang, Lei, and Xiaomin Liu. "Aeroacoustic investigation of asymmetric oblique trailing-edge serrations enlighted by owl wings." *Physics of Fluids* 34, no. 1 (2022): 015113. https://doi.org/10.1063/5.0076272
[11] Li, Dian, Xiaomin Liu, Lei Wang, Fujia Hu, and Guang Xi. "Numerical study on the airfoil self-noise of three owl-based wings with the trailing-edge serrations." *Proceedings of the Institution of Mechanical Engineers, Part G: Journal of Aerospace Engineering* 235, no. 14 (2021): 2003-2016. https://doi.org/10.1177/0954410020988229
[12] Wang, Yong, Kun Zhao, Xiang-Yu Lu, Yu-Bao Song, and Gareth J. Bennett. "Bio-inspired aerodynamic noise control: a bibliographic review." *Applied Sciences* 9, no. 11 (2019): 2224. https://doi.org/10.3390/app9112224
[13] Rao, Chen, Teruaki Ikeda, Toshiyuki Nakata, and Hao Liu. "Owl-inspired leading-edge serrations play a crucial role in aerodynamic force production and sound suppression." *Bioinspiration & biomimetics* 12, no. 4 (2017): 046008. https://doi.org/10.1088/1748-3190/aa7013
[14] Klän, Stephan, Michael Klaas, and Wolfgang Schröder. "The influence of leading edge serrations on the flow field of an artificial owl wing." In *28th AIAA Applied Aerodynamics Conference*, p. 4942. 2010. https://doi.org/10.2514/6.2010-4942
[15] Geyer, Thomas F., Vanessa T. Claus, and Ennes Sarradj. "Silent owl flight: The effect of the leading edge comb on the gliding flight noise." In *22nd AIAA/CEAS Aeroacoustics Conference*, p. 3017. 2016. https://doi.org/10.2514/6.2016-3017
[16] Calkins, Frederick, G. Butler, and James Mabe. "Variable geometry chevrons for jet noise reduction." In *12th AIAA/CEAS Aeroacoustics Conference (27th AIAA Aeroacoustics Conference)*, p. 2546. 2006. https://doi.org/10.2514/6.2006-2546
[17] Sloan, B., J. Wang, Stephen Spence, S. Raghunathan, and D. Riordan. "Aerodynamic performance of a bypass engine with fan nozzle exit area change by warped chevrons." *Proceedings of the Institution of Mechanical Engineers, Part G: Journal of Aerospace Engineering* 224, no. 6 (2010): 731-743. https://doi.org/10.1243/09544100jaero529
[18] Yusoff, H., M. Z. Abdullah, M. Abdul Mujeebu, and K. A. Ahmad. "Effect of skin flexibility on aerodynamic performance of flexible skin flapping wings for micro air vehicles." *Experimental Techniques* 39 (2015): 11-20. https://doi.org/10.1111/ext.12004
[19] Wang, Yong, Kun Zhao, Xiang-Yu Lu, Yu-Bao Song, and Gareth J. Bennett. "Bio-inspired aerodynamic noise control: a bibliographic review." *Applied Sciences* 9, no. 11 (2019): 2224. https://doi.org/10.3390/app9112224
[20] Hussain, Usama, Saif U. Malook, Burhan Shabir, Ozaif Ali, and Sarvat M. Ahmad. "Effect of trailing edge serration on the lift and drag characteristics of NACA0012 airfoil wing." In *35th AIAA Applied Aerodynamics Conference*, p. 4470. 2017. https://doi.org/10.2514/6.2017-4470